

Preparation and Characterization of Sisal Fiber-based Activated Carbon by Chemical Activation with Zinc Chloride

Xincheng Lu, Jianchun Jiang,* Kang Sun, and Xinping Xie

*Institute of Chemical Industry of Forest Products, CAF; National Engineering Laboratory for Biomass Chemical Utilization; Key and Open Laboratory of Forest Chemical Engineering, SFA; Key Laboratory of Biomass Energy and Material, Jiangsu Province; Suojin wucun 16, Nanjing 210042, P.R. China. *E-mail: lhs_ac2011@yahoo.cn*

Received August 25, 2013, Accepted October 11, 2013

Sisal fiber, an agricultural resource abundantly available in china, has been used as raw material to prepare activated carbon with high surface area and huge pore volume by chemical activation with zinc chloride. The orthogonal test was designed to investigate the influence of zinc chloride concentration, impregnation ratio, activation temperature and activation time on preparation of activated carbon. Scanning electron micrograph, Thermo-gravimetric, N₂-adsorption isotherm, mathematical models such as t-plot, H-K equation, D-R equation and BJH methods were used to characterize the properties of the prepared carbons and the activation mechanism was discussed. The results showed that ZnCl₂ changed the pyrolysis process of sisal fiber. Characteristics of activated carbon are: BET surface area was 1628 m²/g, total pore volume was 1.316 m³/g and ratio of mesopore volume to total pore volume up to 94.3%. These results suggest that sisal fiber is an attractive source to prepare mesoporous high-capacity activated carbon by chemical activation with zinc chloride.

Key Words : Sisal fiber, Chemical activation, Activated carbon, Surface characterization, Activation mechanism

Introduction

Activated carbons have been extensively used as excellent adsorbents in a variety of industrial and environmental applications (*i.e.* purification process, removal of organic and metals, and so on), their adsorption capability is shown to be largely controlled by their pore structure, surface area and pore volume.¹⁻³ By IUPAC definition, micropores are pores with radii $r < 2$ nm, mesopores $2 < r < 50$ nm, and macropores $r > 50$ nm. In principle, the activation methods of preparing activated carbons can be divided into two categories: chemical activation and physical activation.⁴ In physical activation, a raw material is first carbonized, and the resulting char is secondarily activated under a flow of suitable gas such as steam, carbon dioxide, air or their mixtures.⁵⁻⁷ In chemical activation, the raw material is impregnated with an activation reagent like H₃PO₄, KOH, ZnCl₂ or their mixtures.^{8,9} Although, H₃PO₄ is shown to be the most environmentally sound chemical for the activation processes, most studies have used zinc chloride due to its effective activating capability. The degradation of cellulose material and the aromatization of the carbon skeleton upon ZnCl₂ treatment result in the creation of the porous structure. The pore structure and adsorption capability of activated carbons are associated with the types of raw material and preparation conditions. In general, activated carbon with both high surface area and porosity, large capacity of adsorption, is desirable.¹⁰

Sisal fiber is an abundantly resource, which is manufactured from the sisal plant. It composes of lignin (8-10%), cellulose (50-65%) and hemi-cellulose (12-20%) which are

suitable for preparing activated carbons. In china, about 3.8 million tons of sisal fiber is produced every year, accounting for 13.8% of total world production. However, there are few reports on preparing activated carbon from sisal fiber and the mechanism of zinc chloride activation. In this paper, activated carbons were prepared from sisal fiber and the activation mechanism of zinc chloride was discussed. Different preparation parameters on the characteristics of activated products were studied to find out the optimum conditions on making activated carbons. Using orthogonal test, the influences of several operating parameters, such as concentration, impregnation ratio, activation temperature and activation time, were investigated. The Langmuir and Freundlich models were used to analysis the adsorption equilibrium. The production of sisal fiber could be of great interest, and the results of this paper can be as helpful reference for sisal fiber agriculture expanding profit.

Experimental

Material. Sisal fiber from Guangxi in China was used as starting material. The as-received sisal fiber was washed to remove dust and then dried and crushed to the length of 1 cm before it was being processed. The proximate analysis of the sisal fiber is shown in Table 1 that showed the fixed carbon of sisal fiber up to 73.4%.

The results of elemental analysis of sisal fiber and sawdust are shown in Table 2. Sawdust is a typical material to produce activated carbon, which has been used widely in industrial production. As shown in Table 2, carbon content of sisal fiber is similar to sawdust, indicting it could be a

Table 1. Proximate analysis of sisal fiber

Sample	Moisture (%)	Ash (%)	Volatile matter (%)	Fixed carbon (%)
Sisal fiber	8.8	4.7	13.1	73.4

Table 2. Elemental analysis of sisal fiber and sawdust %

Samples	C	H	O	S	N
Sisal fiber	42.61	5.63	50.87	0.58	0.31
Sawdust	47.14	5.63	46.1	0.15	0.98

good material to prepare activated carbons.

Preparation of Activated Carbon. Preparation of activated carbon samples from sisal fiber materials, using $ZnCl_2$ chemical activation.^{11,12} We used 10 g sisal fiber material. The particles were impregnated with $ZnCl_2$ at different impregnation ration (w/w) and were kept at 130 °C for 90 min. Pyrolysis was then carried out in a carbonization device. The temperature of the pyrolysis device was raised at 10 °C/min and up to the range of 400-550 °C, and then maintained for 30-90 min. The samples were then washed to remove excess reagent and dried at 110 °C for 3 h. Activated carbons with various specific surface area were prepared.

Orthogonal Test. In preparation of activated carbons using chemical activation, concentration of chemical activation, impregnation ratio, activation temperature and activation time are the key factors, which should be studied. In this paper, orthogonal test was used to determine the optimum conditions for preparation of activated carbons from sisal fiber. Concentration of chemical activation, impregnation ratio, activation temperature and activation time were selected as 4 factors and designed $L_{16}(4^5)$ orthogonal test to study the preparation of activated carbon from sisal fiber. Methylene blue adsorption of sample (q_{MB}) and iodine number of sample (q_{iodine}) were chosen as property index of samples. The orthogonal test is shown in Table 3.

Sample Characterization.

Sample Analysis: The sample analysis (proximate analysis, methylene blue adsorption (q_{MB}) and iodine number (q_{iodine})) was conducted according to test methods of wooden activated carbon (GB/T 12496.1~12496.22-1999). The results of proximate analysis of sample were expressed in terms of moisture, ash, volatile matter and fixed carbon.

Table 3. Factors and levels of the orthogonal text

Levels	Factors			
	A Concentration (%)	B Impregnation ratio (%)	C Activation temp. (°C)	D Activation time (min)
1	45	100	400	30
2	50	150	450	50
3	55	200	500	70
4	60	250	550	90

Specific Surface: Specific surface area (S_{BET}) and porosity of the samples were determined by nitrogen adsorption-desorption isotherms measured in a Micromeritics ASAP 2020 apparatus. Adsorption of N_2 was performed at 77 K. Before analysis, the samples were degassed under N_2 flow at 350 °C for 2 h in a vacuum at 27 Pa. The S_{BET} of the prepared activated carbons was estimated by BET method using N_2 adsorption isotherm data. The micropore volumes were calculated from the amount of N_2 adsorbed at a relative pressure of 0.1, and the mesopore volumes were calculated by subtracting the amounts adsorbed at a relative pressure of 0.1 from those at a relative pressure of 0.95.¹³ To calculate the pore size distribution of samples, the Barret-Joyner-Halenda (BJH) model was employed.

Elemental Analysis: Elemental analysis of samples was performed in a Perkin Elmer 2400 element analyzer. 1 mg sample was burned and the released gases were analyzed. Prior to the flash combustion process, the system was purged with helium carrier gas. Flash combustion was then performed at 2073 K, and the gaseous combustion products were quantified using a thermal conductivity detector. Results were obtained as percentages of carbon and nitrogen, and the oxygen content was determined by difference.

Scanning Electron Micrograph (SEM): The surface morphology of samples were observed using Hitachi S-3400 scanning electron microscope at accelerating voltages of 15 kV. Before observation, the samples were coated with gold in E-1010 Ion sputter.

TG and DTG Analysis: Thermo-gravimetric (TG) experiments were carried out by a thermo-gravimetric analyzer (Netzsch STA 409) in order to determine the pyrolysis behavior of sisal fiber. The dried sisal fiber was subjected to measure in the temperature range of 40-800 °C at heating rate 5 °C/min under flowing of nitrogen gas flow.

Results and Discussion

Preparation of Activated Carbon.

Adsorption Capacity: Activated carbon has good adsorption, which was influenced by preparation conditions. The adsorption capacity of activated carbon depends on not only surface area, but also internal pore structure. The iodine number of activated carbon is related to its micropores while the methylene blue adsorption is related to mesopore. All the four parameters (concentration of chemical activation, impregnation ratio, activation temperature and activation time) in this paper were found to have significant influences on the adsorption capacity of sisal fiber-based activated carbon.

Influence of Activation Temperature on Adsorption Capacity—Figure 1 illustrated the influence of activation temperature on preparation of activated carbon. As seen from Figure 1, the iodine number and methylene blue adsorption increased rapidly with the increase of activation temperature. Activation temperature is the most important parameter in preparing activated carbon, higher activation temperature was good for the pyrolysis of sisal fiber, led to a reduction in the activation energy for the activation reaction

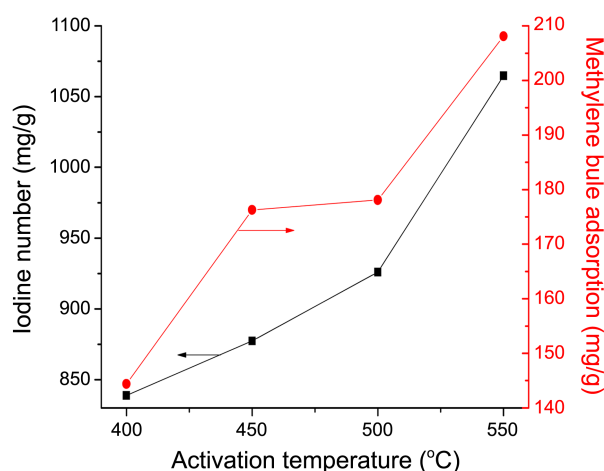


Figure 1. Influence of activation temperature on preparation of activated carbon.

and formed the pores. Meanwhile, higher activation temperature could promote the volatilization of hydroxy group and carboxy group in cellulose with the form of H_2O instead of the form of carbon compound or hydrogen peroxide. But too high temperature will destroy the pore structure, which result in the decrease of micropores and made the activated carbon to exhibit high percentage of mesopores and macropores.

Influence of Activation Time on Adsorption Capacity—Activation time is one of important parameters in the preparing activated carbon. Influence of activation time on adsorption capacity was shown in Figure 2. As shown, the adsorption capacity was increased obviously with the activation time increased from 30 to 70 min. The iodine number and methylene blue adsorption reached the maximum value at 70 min, and then decreased. In polysilysis process, the longer activation time can advance the polysilysis of sisal fiber and the transgression of volatiles, produce pores and surface area, which could enhance the adsorption capacity of activated carbon. However, it is not necessary to prolong the activated time beyond a certain value, because it can increase the

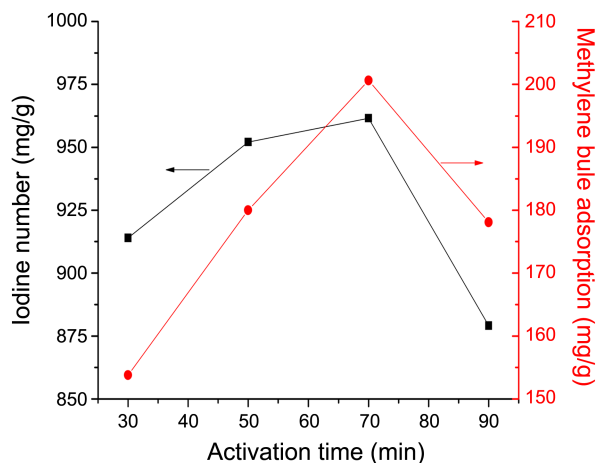


Figure 2. Influence of activation time on preparation of activated carbon.

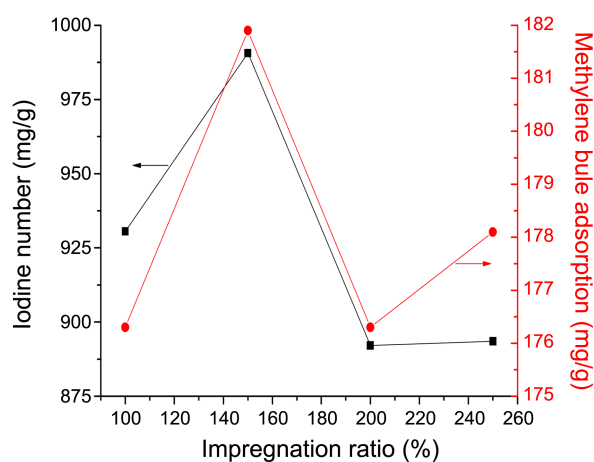


Figure 3. Influence of impregnation ratio on preparation of activated carbon.

evaporation of $ZnCl_2$ and burn off the pore of activated carbons would which decreased the surface area and the adsorption capacity of carbons.¹⁴

Influence of Impregnation Ratio on Adsorption Capacity—Figure 3 shown the influence of impregnation ratio on preparation of activated carbon. It can be seen that adsorption capacity was increased with the increase of impregnation ratio, and then decreased with further the increase of impregnation ratio. The maximum iodine number and methylene blue adsorption were appeared at impregnation ratio of 150%. The extent of chemical activation can significantly alter the characteristics of the produced activated carbons. At low impregnation ratios, $ZnCl_2$ played as dehydrating agent that led to the aromatization of carbon bone, creation and widening of micropores occurred simultaneously; at high impregnation ratios, some $ZnCl_2$ remains in the external part of the carbon particles and widens the porosity by a localized decomposition of the organic matter which enhanced the formation of mesopores and macropores.

Influence of Concentration on Adsorption Capacity—The influence of concentration on preparation of activated

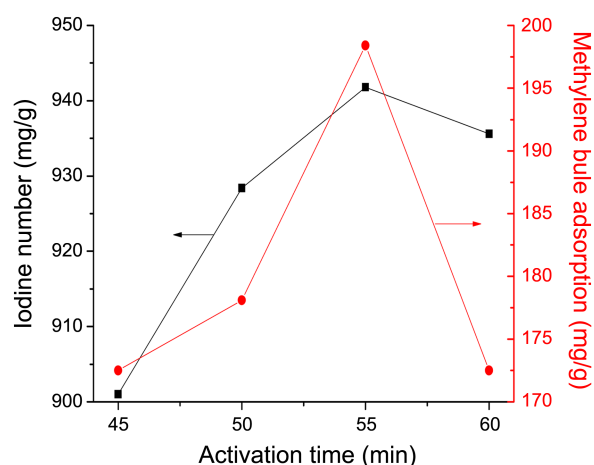


Figure 4. Influence of concentration on preparation of activated carbon.

Table 4. Results and analysis of orthogonal test

No.	A	B	C	D	Property Index	
	Concentration (%)	Impregnation ratio (%)	Activation temp. (°C)	Activation time (min)	q_{MB} (mg*g ⁻¹)	q_{Iodine} (mg*g ⁻¹)
1	1 (45%)	1 (100)	4 (550)	1 (30)	172.5	1082.1
2	1	2 (150)	1 (400)	2 (50)	135	865.9
3	1	3 (200)	2 (450)	3 (70)	187.5	198.8
4	1	4 (250)	3 (500)	4 (90)	195	857
5	2 (50%)	1	1	3	187.5	916.8
6	2	2	4	4	202.5	1029.6
7	2	3	3	1	142.5	844
8	2	4	2	2	180	923.2
9	3 (55%)	1	2	4	165	812.3
10	3	2	3	3	195	1091.7
11	3	3	4	2	225	1108.3
12	3	4	1	1	105	754.8
13	4 (60%)	1	3	2	180	911.1
14	4	2	2	1	195	975.1
15	4	3	1	4	150	817.4
16	4	4	4	3	232.5	1038.9
q_{MB}						
K1	690	705	832.5	615		
K2	712.5	727.5	577.5	720		
K3	690	705	727.5	802.5		
K4	757.5	712.5	712.5	712.5		
k1	172.5	176.3	208.1	153.8		
k2	178.1	181.9	144.4	180		
k3	198.4	176.3	176.3	200.6		
k4	172.5	178.1	178.1	178.1		
R	67.5	22.5	255	187.5		
q_{Iodine}						
K1	3603.8	3722.3	4258.9	3656		
K2	3713.6	3962.3	3354.9	3808.5		
K3	3767.1	3568.5	3509.4	3846.2		
K4	3742.5	3573.9	3703.8	3516.3		
k1	901	930.6	1064.7	914		
k2	928.4	990.6	838.7	952.1		
k3	941.8	892.1	877.4	961.6		
k4	935.6	893.5	926	879.1		
R	163.3	393.8	904	329.9		

carbon was shown in Figure 4. It illustrates that the iodine number and methylene blue adsorption increased with the increase of $ZnCl_2$ concentration, and then decreased with further increase, with the maximum iodine number of about 1064.7 mg/g and the maximum methylene blue adsorption of about 208.1 mg/g. It may be due to the high concentration can provide more Zn^{2+} which could accelerate the hydrolysis and oxidation of fiber and form the pore structure. But the excessive erosion would destroy the pore structure. The methylene blue adsorption was decreased more than the iodine number with concentration increased from 55 to 60%. The same trend was found by Zhang¹⁵ during preparation of activated carbon from sawdust.

Analysis of Orthogonal Test: The range analysis method

was used in this study to analyze the data of orthogonal test and the results were shown in Table 4.

K, k and range (R) were calculated by analyzing on the data of orthogonal test, while K_i is the sum of output response index for certain factor at level i , k_i is the average value of K_i . The R shows the significance of factors' influence on the results. As shown in Table 4, for the q_{MB} property index, the relative of these four factors was in the following order: activation temperature > activation time > concentration > impregnation ratio. The activation temperature was the most prominent factor of the four. It also can be found that the most important factor that influences the q_{Iodine} was activation temperature, followed by impregnation ratio and activation time, and then the concentration.

Considered according to the range analysis, we found that the most important factor in preparation of activated carbon from sisal fiber was activation temperature, then activation time, followed by impregnation ration, and the last was concentration.

Process Optimization: The main aim of this paper was to find the optimum preparation conditions preparing activated carbon from sisal fiber. In the orthogonal test method, the change of every level for one factor was not effected by other factors. Therefore, the optimum preparation conditions can be obtained by combining the best level of each factor. As shown in Table 4, the optimum preparation conditions of preparing activated carbon from sisal fiber were: the concentration of ZnCl_2 55%, impregnation ration 1:1.5, activation temperature 550 °C and activation time 70 min.

Surface Area and Pore Size Distribution. The sample that prepared under the optimum preparation conditions was identified as AC. The Brunauer-Deming-Deming-Teller (BDDT) theory, the basis of the modern IUPAC classification, was used in this study to characterize the surface area and pore structure of AC.

Adsorption-desorption Isotherms: The analysis of N_2 -adsorption isotherm of AC was shown in Figure 5, which provided an approximate assessment of the pore size distribution. As shown in Figure 5, the first nitrogen uptake was significant in the low-pressure region where $p/p_0 < 0.2$ and the second knee generated in the range of $p/p_0 > 0.8$. This observed characteristics indicated the occurrence of the process of pore widening and a significant development of the mesoporosity. Aranovich and Donohue¹⁶ found that this type of isotherm was attributed to the mesoporous solids. The hysteresis loop is a characteristic feature of this kind of isotherms, associating with capillary condensation occurring in mesopores and with the limiting uptake occurring at high relative pressure.

The hysteresis loop of isotherms is associated with the pore shape and pore structure of materials. The N_2 -adsorption-desorption isotherm of AC was shown in Figure 6. As shown, the N_2 -adsorption-desorption isotherm of AC belongs

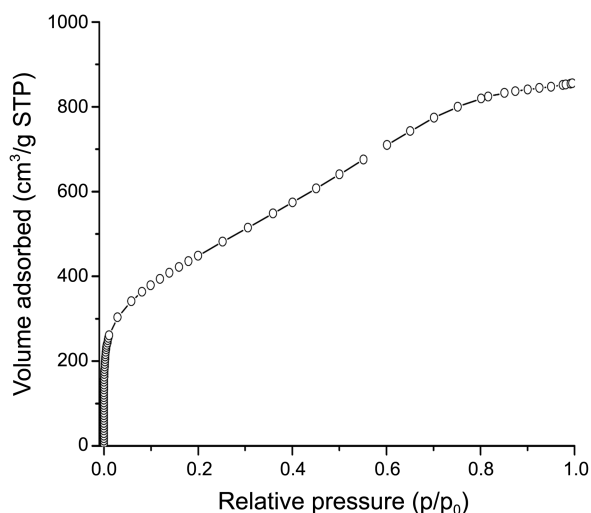


Figure 5. N_2 -adsorption isotherm of AC.

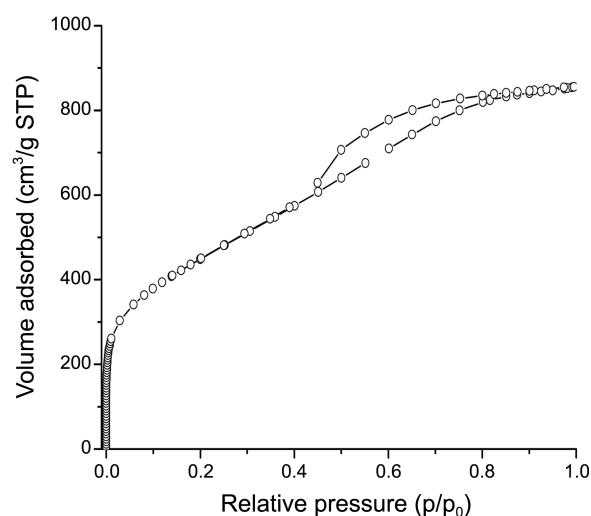


Figure 6. N_2 -adsorption-desorption isotherms of AC.

to type IV, which suggested it was mesoporous material. The type of hysteresis loop was H4, suggesting the existence of slit-shaped pores.

Analysis of the Pore Structure: Two empirical methods, t-plot and H-K equation, were used to estimate the micropores volume. Figure 7 presented t-plot constructed for AC. Since a linear t-plot represents a non-pore carbon, the observed deviation from linearity suggested the presence of micropore and mesopore structure. The y-axis represents the amount of N_2 adsorbed, and x-axis represents the t values (the thickness of adsorbed layer). As shown in Figure 7, t-plots of AC had elevated greater slopes at higher t regions, which indicated the formation of the mesopore structure. Due to the contribution of the mesopores, the AC micropores volume was lower. The calculated micropores volume from t-plots was shown Table 5.

To understand the micropore size distribution of AC, H-K equation was used. Considered the interaction force between adsorbates and adsorbents, H-K equation can response the adsorption process objectively. The result of H-K equation

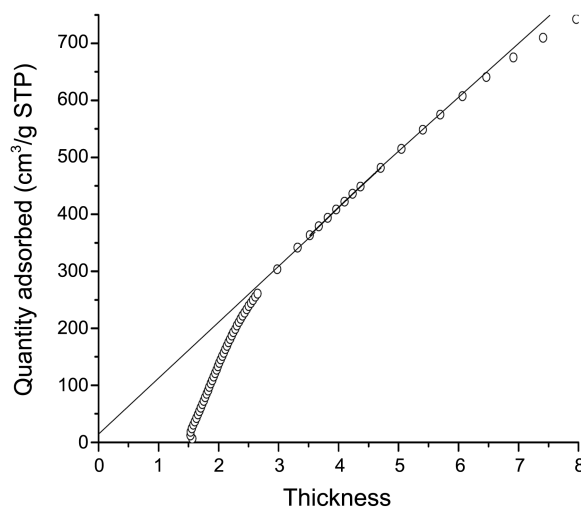
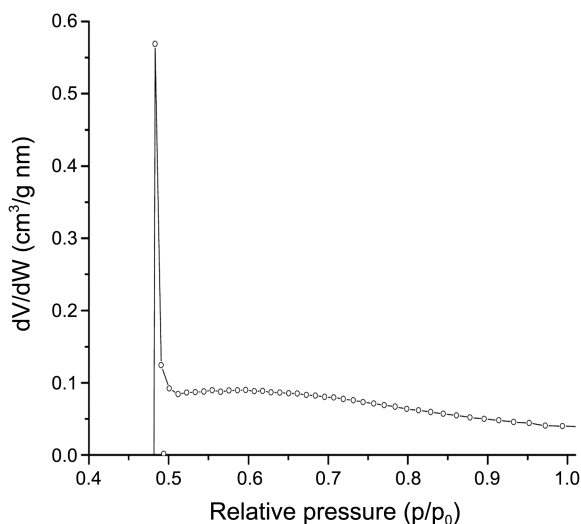


Figure 7. Representative t-plots of AC.

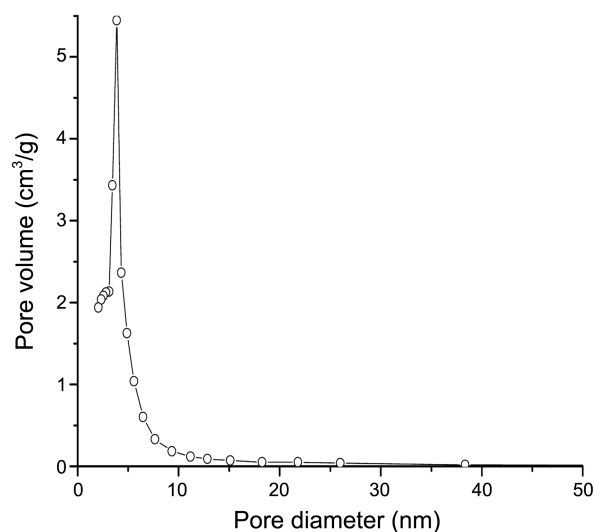
Table 5. Micropore volume of the AC

Sample	Micropore area (m ² /g)	External surface area (m ² /g)	Micropore volume (m ³ /g)
AC	79	1549	0.017

**Figure 8.** Microporous size distribution of AC by H-K equation.

was shown in Figure 8 and indicated that micropore was mainly distributed in 0.51–1.0 nm. The distribution of micropore was single dispersion and the peak represented predominant pore sizes appeared at 0.49 nm. Calculated from H-K equation, the average pore width of micropores was 0.68 nm.

Analysis of the Pore Size Distribution: The micropore and mesopore size distribution were evaluated using Barret, Joyner and Halenda (BJH) method and the result was shown in Figure 9. As shown, it can be seen that the pore sizes of AC were mainly mesopores. The peak that represented the predominant pore size appeared at 5 nm, which suggested that pore diameter for the mesoporous carbons. This result agreed well with the Gonzalez-Serano results that an excess

**Figure 9.** Pores size distribution of AC.**Table 6.** Surface area, pore volume, and average diameter of AC

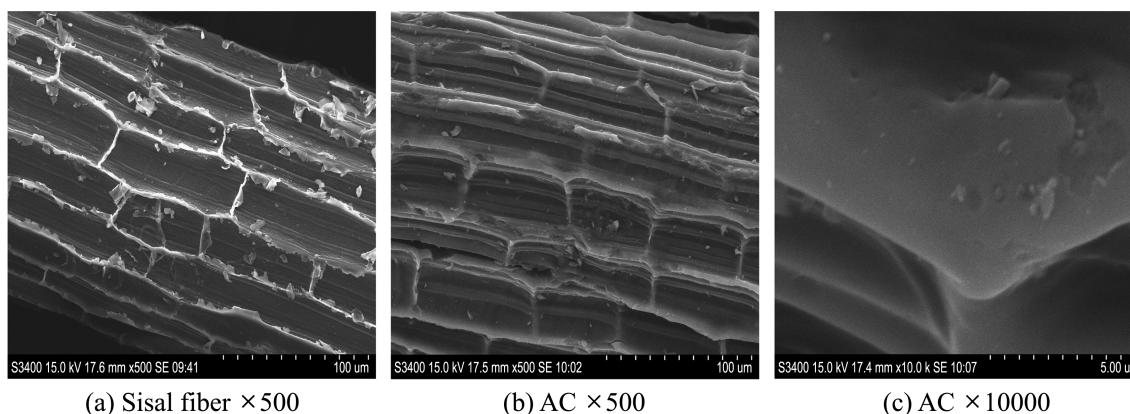
Sample	S_{BET} (m ² /g)	V_{tot} (m ³ /g)	V_{mic} (m ³ /g)	V_{mes} (m ³ /g)	$(V_{\text{mes}}/V_{\text{tot}})$ (%)	D (nm)
AC	1628	1.316	0.017	1.241	94.3	3.23

* $V_{\text{mes}}/V_{\text{tot}}$: Ratio of mesopore volume to total pore volume

amount of ZnCl₂ could enhance the process of the pore widening and transform the micropore to mesopore.¹⁷

Specific surface area (S_{BET}), total pore volume (V_{tot}), micropores volume (V_{mic}), mesopores volume (V_{mes}) and average diameter (D) of AC was tabulated in Table 6. The maximum BET surface area was 1628 m²/g, and total pore volume was 1.316 m³/g. Ratio of mesopores volume to total pore volume up to 94.3%, suggesting it is a good mesoporous material which has uniform-pore distribution. Gregg and Sing¹⁸ found that the mechanism of the adsorption in very fine pore is controlled mainly by the pore filling processes rather than the surface coverage. Therefore, this AC could be used as good adsorption material.

Scanning Electron Micrograph (SEM). The microstructure of the sisal fiber and AC were presented in Figure 10. For

**Figure 10.** SEM of sisal fiber and AC.

the sisal fiber, the micrograph exhibited clearly bundle structure, which was a good characterization for preparing activated carbons using chemical activation, because activating agents can easily contact with the inside surface of material. The micrograph of AC showed clean surface with greater porosity and the bundle structure has been partly broken, which was due to the eroded by activating agents in the activation process. The pore structure of AC can provide high specific area and enhance the adsorption ability of activated carbons. The white particles presenting on the surface of AC were called ash content, which may fill or block some portion of the micropore.

TG and DTG Analysis. Figure 11 shows the TG-DTG curves of sisal fiber and sisal fiber impregnated with ZnCl_2 in a N_2 atmosphere and at a $10\text{ }^\circ\text{C}/\text{min}$ heating rate. It can be seen from Figure 11(a), the thermal decomposition behavior of sisal fiber is in the first stage from 50 to $110\text{ }^\circ\text{C}$; the second stage from 200 to $350\text{ }^\circ\text{C}$. Weight loss happened in

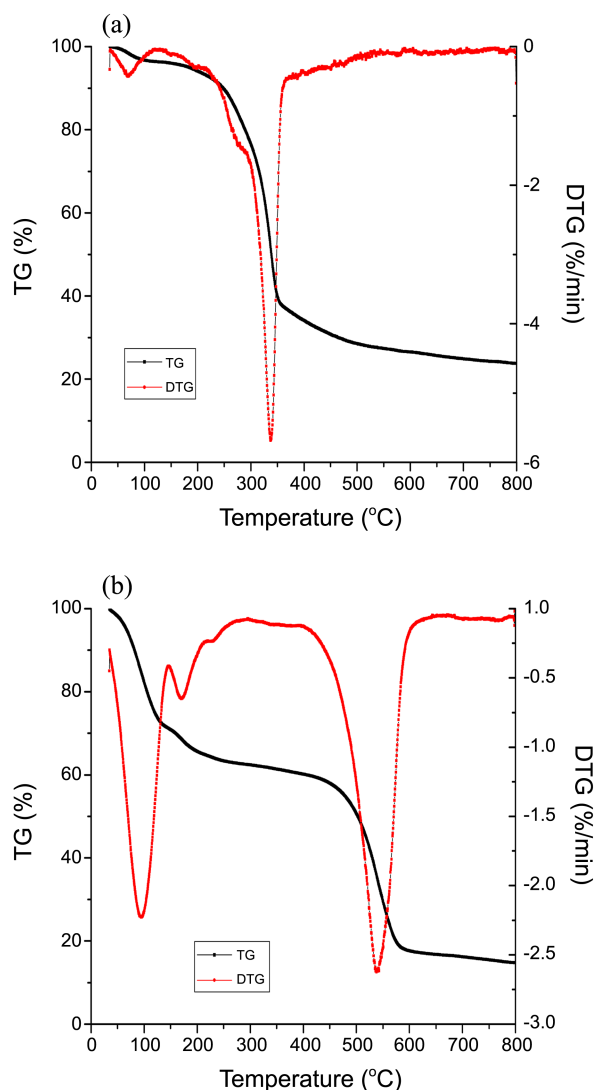


Figure 11. TG/DTG curves for sisal fiber and sisal fiber impregnated with ZnCl_2 . (a) Sisal fiber; (b) Sisal fiber impregnated with ZnCl_2 .

first stage because of the evaporation of moisture which was remained in sisal fiber. In this stage, DTG curve shows a little drop, because the sisal fiber needs heat to evaporate the remaining water. The second stage presented a significant weight loss due to the released of volatile. From $200\text{ }^\circ\text{C}$, hemi-cellulose started to decompose and released heat while cellulose began to decompose and release heat at $240\text{ }^\circ\text{C}$. When the temperature was about $330\text{ }^\circ\text{C}$, hemi-cellulose and cellulose decomposed and produced abundant organic compounds, such as wood tar, methanol and ketone, which would vaporize by adsorbed heat. There are numerous hemi-cellulose and cellulose in sisal fiber, so the peak of DTG curve was apparent in this stage.

As shown in Figure 11(b), the pyrolysis process of sisal fiber was changed after impregnated with ZnCl_2 . The thermal decomposition behavior of sisal fiber impregnated with ZnCl_2 was divided into two stages: the first stage from 50 to $200\text{ }^\circ\text{C}$ and the second stage from 450 to $570\text{ }^\circ\text{C}$. Compared to Figure 11(a), weight loss in the first stage was more significant and DTG curve presented two peaks. As one kind of Lewis acid, ZnCl_2 could promote the polymerization of aromatics and change the pyrolysis process of material which advance the decomposition of hemi-cellulose and cellulose and form the pore structure.¹⁹ Therefore, weight loss in the first stage due to the evaporation of moisture and the decomposition of hemi-cellulose and cellulose. In the second stage, sisal fiber reacted with activating reagent. When temperature was about $450\text{ }^\circ\text{C}$, ZnCl_2 eroded and reacted with sisal fiber and produced high surface area and huge pore volume which resulted weight loss and heat releasing. At $600\text{ }^\circ\text{C}$, TG and DTG curves reached at base line, pyrolysis reaction was over and the residue was just graphite carbon and ash. So, the best activation temperature can be obtained in the range from 450 to $600\text{ }^\circ\text{C}$ for preparing sisal fiber activated carbon.

Conclusions

The results of this paper showed that sisal fiber can be successfully converted into activated carbon with high surface area and huge pore volume by chemical activation using ZnCl_2 . Activation conditions has a significant influence on preparation of activated carbon. The optimum preparation conditions of preparing activated carbon from sisal fiber were: the concentration of ZnCl_2 55%, impregnation ration 1:1.5, activation temperature $550\text{ }^\circ\text{C}$ and activation time 70 min. It was also found that the activation temperature was the most prominent factor, then activation time, followed by impregnation ration, and the last was concentration. As an activator, ZnCl_2 changed the pyrolysis process of sisal fiber, advanced the decomposition of hemi-cellulose and cellulose, prevented blockage of pore by tar and formed the mesopores. In addition, surface area and mesoporous were well developed in this prepared activated carbon, may be further developed as potential adsorbents for purification of water and chemical processing. Thus preparing activated carbon from sisal fiber is a promising work.

Acknowledgments. This research is financially supported from the projects in forestry public benefit research sector (201404610) and the national science& technology pillar program in the eleventh five-year plan period (2009BADB1B03). And the publication cost of this paper was supported by the Korean Chemical Society.

References

1. Boppart, S.; Ingle, L.; Potwora, R. J.; Rester, D. O. *Chem. Process* **1996**, *59*, 19.
 2. Lu, X. C.; Jiang, J. C.; Sun, K.; Xie, X. P.; Hu, Y. M. *Appl. Surf. Sci.* **2012**, *258*, 8247.
 3. Lu, X. C.; Jiang, J. C.; Sun, K.; Cui, D. D. *Appl. Surf. Sci.* **2011**, *258*, 1656.
 4. Sun, K.; Jiang, J. C. *Biomass Bioenerg.* **2010**, *34*, 539.
 5. Zhang, T. Y.; Walawender, W. P.; Fan, L. T.; Fan, M. H.; Daugaard, D.; Brown, R. C. *Chem. Eng. J.* **2004**, *105*, 53.
 6. Haykiri-acma, H.; Yaman, S.; Kucukbayrak, S. *Energ. Convers. Manage.* **2006**, *47*, 1004.
 7. Yang, T.; Lua, A. C. *J. Colloid Interf. Sci.* **2003**, *267*, 408.
 8. Hayshi, J.; Toshihide, H.; Isao, T.; Katsuhiko, M.; Fard, N. A. *Carbon* **2002**, *13*, 40.
 9. Guo, Y. P.; Rockstraw, H. *Micropor. Mesopor. Mat.* **2007**, *100*, 12.
 10. Zhong, Z. Y.; Yang, Q.; Li, X. M.; Luo, K.; Liu, Y.; Zeng, G. M. *Ind. Crop. Prod.* **2012**, *37*, 178.
 11. Reinoso, F. R.; Buss, G. Y. European Patent EP0329251, 1993.
 12. Molina-Sabio, M.; Rodriguez-Reinoso, F. *Colloid Surface A.* **2004**, *241*, 15.
 13. Rodriguez-Reinoso, F.; Lopez-Gonzalez, J. De. D.; Berenguer, C. *Carbon* **1982**, *20*, 513.
 14. Li, W.; Zhang, L. B.; Peng, J. H.; Li, N.; Zhu, X. Y. *Ind. Crops. Prod.* **2008**, *27*, 341.
 15. Zhang, H. P.; Ye, L. Y.; Yang, L. C. *Materials Sci. Techn.* **2006**, *14*, 43.
 16. Arabovich, G.; Donohue, M. *J. Colloid Interf. Sci.* **1998**, *200*, 273.
 17. Gonzalez-Serano, E.; Cordero, T.; Rodriguez-Mirasol, J.; Rodriguez, J. J. *Ind. Eng. Chem. Res.* **1997**, *36*, 4832.
 18. Gregg, S. J.; Sing, K. S. W. Academic Press: 1982; pp 257-283.
 19. Ahmadpour, A.; Do, D. D. *Carbon* **1997**, *35*, 1723.
-